Water-loaded plasmonic stripe integrated with Si_3N_4 waveguide using gold and CMOS compatible metals

A. Manolis[1], G. Dabos[1], D. Ketzaki[1], E. Chatzianagnostou[1], N. Pleros[1], L. Markey[2], J.C. Weeber[2], A. Dereux[2], A.L. Giesecke[3], C. Porschatis[3], B. Chmielak[3] and D. Tsiokos[1]

[1] Department of Informatics - Center for Interdisciplinary Research and Innovation, Aristotle University of Thessaloniki, Greece, Tel: +302310990588, e-mail: dtsiokos@csd.auth.gr,

[2]Laboratoire Interdisciplinaire Carnot de Bourgogne, CNRS-Université de Bourgogne, Dijon, France

[3]AMO GmbH, Advanced Microelectronic Center Aachen (AMICA), Otto-Blumenthal-Strasse, Aachen, Germany,

ABSTRACT

In this work, we report the integration of low loss Si_3N_4 waveguides with water-loaded thin plasmonic stripes. Experimental measurements revealed a photonic to plasmonic insertion loss of 2.3dB per transition and a propagation length of 75μm at 1550nm when using gold as plasmonic metal. With the aid of numerical simulations we also demonstrate how CMOS compatible metals may be used to realize such structures at low cost. The proposed waveguide scheme holds promise as an optical transducer in future plasmonics-augmented biosensors.

Keywords: Surface plasmons, thin-film plasmonics, silicon nitride, photonic integrated circuits. CMOS metals.

1. INTRODUCTION

Plasmonic technology may revolutionize photonic-integrated-circuits (PICs), unleashing unprecedented performance breakthroughs. Harnessing the unique capability of plasmonic waveguides to guide light at metal surfaces can offer sub-wavelength confinement and increased light–matter interaction at the metal surface [1]. However, the inherent high propagation losses of SPP waveguide configurations impede their broad utilization in more complicated PICs. To lower this barrier, plasmonic structures may be selectively co-integrated with low-loss photonic waveguides therefore minimizing chip losses coming from plasmonic sections while reaping the benefits of guiding light over metal surfaces. Merging plasmonics with photonics in a common integration platform has been so far demonstrated in a range of waveguide configurations and functional devices [2]-[5] however, only a limited number of plasmo-photonic interface structures has been proposed when plasmonic propagation in aqueous environment is required [4], [5] as is typically the case when biochemical sensing applications are targeted. In this paper, we demonstrate the co-integration of water-loaded gold-based plasmonic stripe waveguide with a Si_3N_4 waveguide, utilizing a butt-coupled interface for potential application in future biosensing applications. Following the same design methodology we evaluate the performance of the proposed structures when relying on CMOS-compatible metals such aluminium and copper.

2. GOLD-BASED PLASMONIC STRIPE ON Si_3N_4

2.1 Design and simulation

Figure 1(a) illustrates the proposed plasmo-photonic structure. A Si_3N_4 photonic waveguide and a gold-based plasmonic stripe waveguide are interfaced in a butt coupled scheme via photonic linear tapers. The test structure exploits Si_3N_4 TM grating couplers (GCs) to achieve coupling in and out of the chip [6]. Figure1(b) depicts a more detailed side-view geometry of the proposed interface. The main challenge of interfacing the silicon nitride and the gold stripe waveguides was to spatially match photonic and plasmonic mode profiles. Our design process was based on the optimization of two parameters: Longitudinal Offset (LO) and Vertical Offset (VO) between the photonic and plasmonic waveguide facets, as shown in Fig.1(b). LO and VO were optimized via numerical simulations, in terms of coupling efficiency, to the values of 500nm and 400nm respectively, as described in [8].

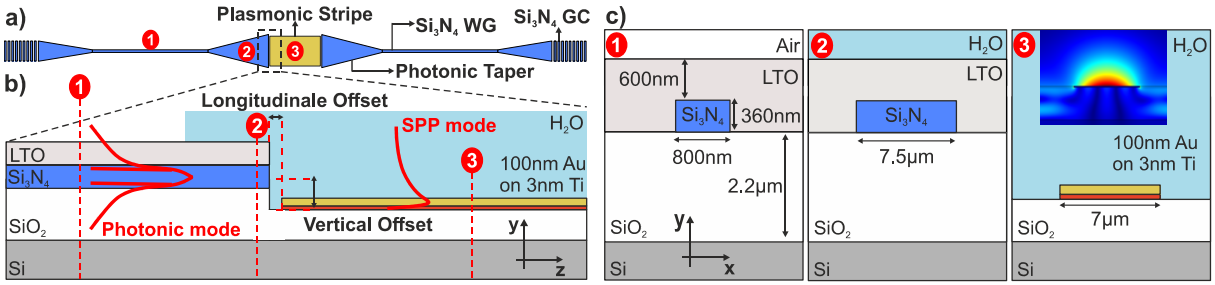

Figure 1. (a) Schematic representation of the proposed interface structure. (b) Sideview of the proposed interface illustrating Vertical Offset (VO) and Longitudinal Offset (LO) parameters. (c) Cross-section and dimensions of the photonic and the plasmonic waveguides.

The different cross-sections across the structure including the photonic waveguide (1) the taper end facet (2) and the plasmonic waveguide (3) are depicted in Fig.1(c). A 360nm × 800nm Si_3N_4 photonic waveguide core is cladded with 600nm of LTO on a 2.2μm thick SiO_2 substrate layer (Fig.1(c)(1)). The photonic waveguide is linearly tapered to 7.5μm width forming a photonic taper waveguide (Fig.1(c)(2)) which is interfaced with a 100nm × 7μm plasmonic stripe exposed to the surrounding medium. The plasmonic waveguide resides on a Ti layer located between the gold film and the SiO_2 layer (Fig.1(c)(3)). As illustrated in Fig.1(c), the plasmonic waveguide and the photonic taper are surrounded by water in order to evaluate coupling performance in conditions encountered in potential biosensing-related applications. Numerical simulations for the proposed structure predicted a coupling loss equal to 2.2dB and an L_{SPP} reaching 86μm at 1550nm [7].

2.2 Fabrication and characterization

For the fabrication of the proposed interface structure, a standard 6'' silicon wafer with 2.2μm of thermally grown SiO_2 has been employed as substrate. The Si_3N_4 waveguide was deposited in low pressure chemical vapor deposition process (LPCVD). Optical projection lithography with a CANON i-line stepper tool was used to define markers, waveguides and GCs. Reactive-ion-etching (RIE) based on CHF_3 and He chemistry was exploited for the structure transfer of the waveguides. Following this, 600nm of SiO_2 were deposited in a low temperature LPCVD furnace (LTO). A subsequent annealing process for several hours at 1000°C minimized hydrogen content and absorption of the LTO cladding to reduce the waveguide propagation losses. Afterwards, cavities for the plasmonic material were defined by the i-line stepper tool and etched 1.36μm deep through LTO, Si_3N_4 and SiO_2 as well by RIE with CHF_3 and He chemistry. In the final fabrication stage, the metallic plasmonic stripes were deposited into the cavities by a lift-off process using e-beam lithography, thermal evaporation of gold and lift-off dissolution. A very thin (3nm) titanium layer was deposited by e-gun evaporation prior to gold for an improved adhesion of gold on the sample. SEM images of the fabricated structure are shown in Figure 2(a).

Characterization measurements were carried out to evaluate propagation losses as well as the photonic to plasmonic coupling loss. Broadband measurements were carried out by sweeping the wavelength of a tunable laser source from 1500nm to 1580nm to launch light into Si_3N_4 GCs of the cut-back sections. By performing linear fitting process on the measured data, we calculated 0.058dB/μm propagation losses at 1550nm corresponding to an L_{SPP} equal to 75μm, showing good agreement with the simulation predicted value of 86μm. Blue scatter points in Fig.2(b) indicate the broadband operation of the structure by maintaining similar propagation losses measured for a wavelength range over 80nm. Red scatter points in Fig.2(c) illustrate the calculated photonic-to-plasmonic coupling loss, revealing broadband operation with a value of 2.3dB at 1550nm, for a single transition adequately matching the value of 2.2dB predicted numerically.

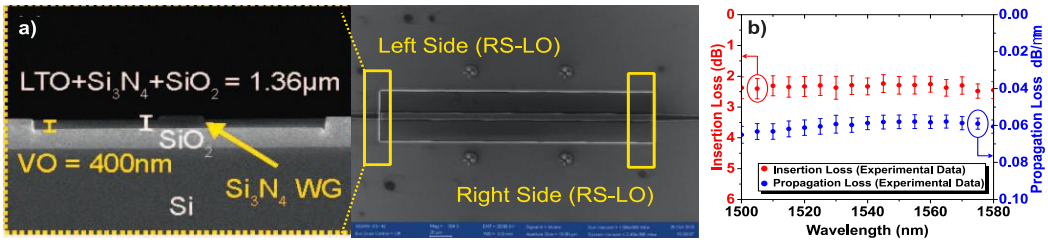

Figure 2. (a) SEM images of the interface structure in cross section and stripe top view. (b) Broadband experimental data for the insertion and propagation loss.

3. MODELLING OF CMOS-COMPATIBLE STRUCTURES

Successful matching of the numerical predictions with the experimental results for the Au-based plasmonic structure allowed us to use the same simulation methodology for the design of CMOS compatible plasmonic waveguides by replacing gold with low cost Aluminium (Al) and Copper (Cu). As in the case of the Au-based thin-film configuration reported in [7], the design study for the CMOS-based thin-film structure begins with a 2D eigenvalue analysis on the cross-sections of the waveguides under investigation. The coupling mechanism for this end-fire structure is expected to be governed by the same principles as the case of Au, so spatial mode matching should be achieved in order to efficiently transfer the light from the photonic to the plasmonic waveguide. The power overlap integral analysis led to similar results for the dimensions of the two waveguide structures under study (Si_3N_4 photonic and thin-film plasmonic waveguide) both for Al- based (n_Al=1.42-15.1i) and Cu-based (n_Cu=0.26-9.8i) [9] plasmonic metals.

To have a fair comparison between the different metal materials the same dimensions for the Si_3N_4 photonic and Au-based thin-film plasmonic waveguides have been retained i.e. 360nm×7.5μm for the Si_3N_4 photonic core and 100nm×7μm for the metallic thin-film stripe. It is shown that, for these dimensions at the wavelength of interest (1550nm), the fundamental TM plasmonic mode is supported by both the Al- and the Cu-based thin-film waveguides having an electric field distribution similar to the one of the Au-based structure. The effective indices derived from this 2D eigenmode study were neff_Al=1.312-0.00196i and neff_Cu=1.319-0.00156i corresponding to propagation lengths (L_{SPP}) of 63μm and 79μm for the Al- and the Cu-based structure, respectively.

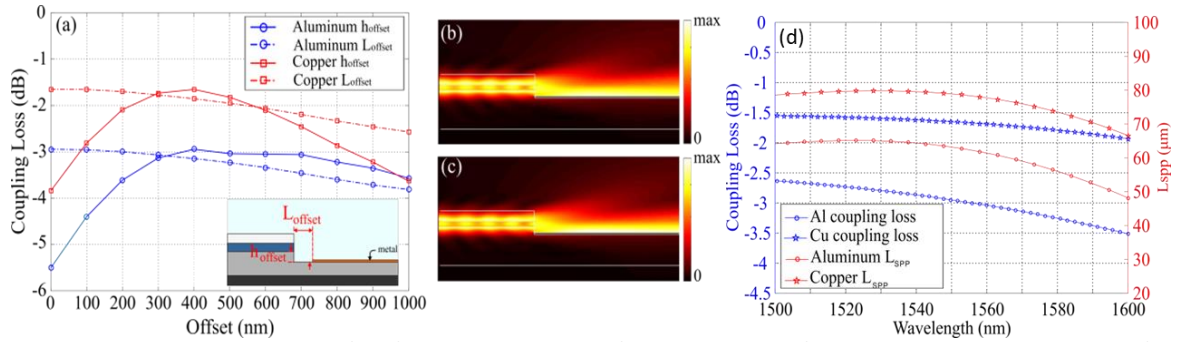

Figure 3. (a) Coupling loss versus h_{offset} for a fixed L_{offset}=0μm and L_{offset} for the optimum h_{offset} for both CMOS metals. (b), (c) Electric field distribution along the light propagation direction for optimal (L_{offset} =0nm, h_{offset} =400nm) Al-based structure and Cu-based structure respectively, (d) Coupling loss (blue curves) and plasmonic propagation length (red curves) versus wavelength for the end-fire configurations.

An end-fire interface configuration as the one depicted in the inset of Figure 3(a) was analysed by means of 3D FDTD numerical simulations adopting Al and Cu as the plasmonic metal material. The effect of both vertical (h_{offset}) and lateral (L_{offset}) offset distances on induced coupling loss of the plasmo-photonic interface has been investigated. Figure 3(a) shows the results of this numerical analysis both for Al and Cu. For both the Al- and the Cu-based structures the variation of coupling loss with respect to h_{offset} exhibits a local minimum around h_{offset}=400nm corresponding to stronger coupling. At the same time, the variation of coupling loss versus L_{offset} exhibits a monotonically decreasing behavior signifying that the minimum achieved coupling loss is obtained for L_{offset}=0 for both CMOS metal materials yet coupling excess loss remains always below 1dB for an L_{offset} up to 1μm. Moreover, the end-fire structure based on Cu seems to have better performance in terms of coupling efficiency when compared to Al. As such, the minimum achieved coupling loss for L_{offset} =0 and h_{offset} =400nm has been calculated at -2.94dB and -1.65dB for Al and Cu, respectively. Figures 3(b) and 3(c) illustrate the electric field distributions along the light propagation direction for both CMOS metals.

The broadband functionality of the CMOS end-fire structures was also investigated in the wavelength region 1500nm-1600nm. As illustrated in Fig. 3(d), small deviations in coupling loss and in L_{SPP} are observed for both metals when the wavelength deviates from 1550nm to 1600nm rendering the CMOS end-fire configurations functionally tolerant in this wavelength range indicating again a 1-dB bandwidth greater than 100nm.

4. CONCLUSIONS

We demonstrate a butt-coupled scheme for efficiently integrating low loss Si_3N_4 waveguides and water-loaded plasmonic stripes with experimentally measured insertion loss of 2.3dB per transition and an Lspp of 75μm at 1550nm. The same design methodology was used to draw a clear path for replacing noble metals in plasmonics with low cost, CMOS-compatible metals such as Al or Cu for mass manufacturing integrated biosensors.

ACKNOWLEDGEMENTS

This work was supported by the European H2020, PLASMOfab project (Co. No. 688166).

REFERENCES

[1] D. K. Gramotnev and S. I. Bozhevolnyi, Plasmonics beyond the diffraction limit, *Nat. Photonics* vol.4 pp. 83–91, 2010.

[2] O. Tsilipakos, et al, Interfacing dielectric-loaded plasmonic and siliconphotonic waveguides: theoretical analysis and experimental demonstration, *IEEE J. Quantum Electron*. vol.48, pp. 678–687, 2012.

[3] C. Delacour et al, Efficient directional coupling between silicon and copper plasmonic nanoslot waveguides: toward metal− oxide−silicon nanophotonics, *Nano Lett*., vol. 10, pp. 2922-2926, 2010.

[4] Xu Sun et al., High-sensitivity liquid refractive-index sensor based on a Mach-Zehnder interferometer with a double-slot hybrid plasmonic waveguide, *Opt. Express*, vol.23, pp.25688-25699, 2015.

[5] B. Y. Fan et al, Refractive index sensor based on hybrid coupler with short-range surface plasmon polariton and dielectric waveguide, *Appl. Phys. Lett*. vol. 100, 111108, 2012.

[6] G. Dabos et al., TM grating coupler on low-loss LPCVD based Si_3N_4 waveguide platform, *Opt. Com.*, vol. 405, pp. 35-38, 2017.

[7] G. Dabos et al., Butt-coupled interface between stoichiometric Si_3N_4 and thin-film plasmonic waveguides, *in Proc. SPIE P.W.*, p.10106-41, San Francisco, USA, 2017.

[8] G. Dabos et al., Plasmonic stripes in aqueous environment co-integrated with Si3N4 photonics, *in IEEE Photonics Journal*, vol. PP, no. 99, pp. 1-1.

[9] J.-C. Weeber, et al, Characterization of CMOS metal based dielectric loaded surface plasmon waveguides at telecom wavelengths, *Opt. Express*, vol. 25, pp. 394–408, 2017.